DFT Studies on the Thermal Activation of Molecular Oxygen by Bare $[Ni(H)(OH)]^+$

by **Xinhao Zhang**[a]), **Maria Schlangen**[a]), **Mu-Hyun Baik**[b]), **Yavuz Dede**[b]), and **Helmut Schwarz***[a])

[a]) Institut für Chemie, Technische Universität Berlin, Straße des 17. Juni 135, DE-10623 Berlin (fax: +49-30-314-21102; e-mail: Helmut.Schwarz@mail.chem.tu-berlin.de)

[b]) Department of Chemistry, Indiana University, 10th Street, Bloomington, IN 47405, USA

Dedicated to Professor *Rudolf Zahradník* on the occasion of his 80th birthday

An extensive density-functional theory (DFT) study has been conducted to shed light on the mechanisms of the recently reported gas-phase ion-molecule reactions of mass-selected $[Ni(H)(OH)]^+$ with O_2 (M. Schlangen, H. Schwarz, *Helv. Chim. Acta* **2008**, *91*, 379). Except for the liberation of OH from the encounter complex, all of the other highly atom-specific processes can be explained in a consistent manner.

Introduction. – For the *in vitro* metal-mediated activation of molecular oxygen, numerous efficient catalytic systems, often based on Pd^{II} compounds, are available[1]). As to the mechanism, several variants have been proposed[1])[2])for the reactions of O_2 with, *e.g.*, Pd^{II} hydride complexes (*Scheme 1*; M = Pd). While formation of genuine Pd^{II} hydroperoxides has been demonstrated experimentally to occur [3], for nearly all systems studied it has been difficult to mechanistically unambiguously characterize how triplet oxygen interacts with singlet Pd^{II} hydrides to generate singlet Pd^{II} hydroperoxides. The latter may serve as intermediates for the catalytic oxidations of various substrates by O_2 or the *in situ* generation of H_2O_2. The favored mechanistic scenarios suggested involve a direct insertion of O_2 into the Pd^{II}–hydride bond, *e.g.*, *via Path a* (*Scheme 1*) [4], or the interaction of O_2 with a Pd^0 complex (*Path b*), generated *via* reductive elimination of HX from $L_nM(H)X$. Detailed computational studies, which address also some extent aspects of the intriguing spin conversions from triplet to singlet, as well as experimental findings imply that, depending on the nature of the ligand L and the counterion X, in addition to *Scheme 1*, quite a few mechanistic alternatives are conceivable [1][2][5]. In particular, for the oxidation of the other late transition-metal hydrides (*e.g.*, with M = Rh, Pt, Co, and Ir) radical chain autooxidations seem to play a role [6]. Given the complexity of the solution experiments and the manifold of conceivable mechanistic variants, experimental investigations of structurally more simple (model) systems under well-defined conditions were recommended to resolve the currently existing dilemma [1][2][5].

---

1) For review and highlight articles, see [1].

2) For a detailed discussion of mechanistic aspects, see [2].

© 2009 Verlag Helvetica Chimica Acta AG, Zürich

Scheme 1

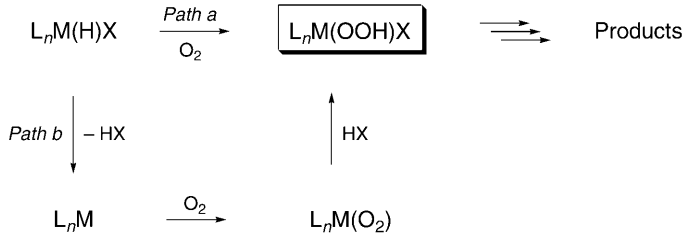

In the context of gas-phase molecular oxygen-activation studies aimed at uncovering intrinsic mechanistic features of this important class of processes, numerous ionic systems have been investigated [7]. With regard to the above described mechanistic questions in the reactions of metal hydride/O_2 couples, we decided to explore the thermal reactions of molecular oxygen with structurally rather simple transition-metal hydride ions $[M(H)(OH)]^+$ in the gas phase. These formal M^{III} cations were chosen for the quite extraordinary reactivity some of them had exhibited; *e.g.*, $[Ni(H)(OH)]^+$ brings about efficient, thermal activation of CH_4 (*Eqn. 1*). In contrast, although thermochemically feasible, the analogous Fe^{III} and Co^{III} hydrides do not react according to *Eqn. 1* [8].

$$[Ni(H)(OH)]^+ + CH_4 \rightarrow [Ni(CH_3)(OH)]^+ + H_2 \quad (1)$$

For the $[Ni(H)(OH)]^+/O_2$ system, it turned out that, under single-collision conditions, rather efficient ($k_{rel} = 22\%$ with regard to collision rate) oxidation occurs at room temperature (*Eqn. 2*) [9].

$$[Ni(H)(OH)]^+ + O_2 \rightarrow \begin{cases} [Ni,O,H]^+ + HO_2 & 7\ \% \\ [Ni,O_2]^+ + H_2O & 34\ \% \\ [Ni,H,O_2]^+ + HO & 37\ \% \\ [Ni,H_2,O_2]^+ + O & 22\ \% \end{cases} \quad (2)$$

While the actual structures of the ionic products generated remained by and large unknown, details about the origin of the neutral molecules liberated in the course of the ion–molecule reaction could be extracted from labeling experiments [9], which revealed an extraordinarily high selectivity (*Fig. 1*). For instance, in the formation of HO_2, the OH group of $[Ni(H)(OH)]^+$ is not involved at all, and the production of H_2O follows a path in which the O-atom is exclusively provided by molecular oxygen. Similarly, the OH radical contains the H-atom of the Ni–H bond, and its O-atom originates from O_2; obviously, the OH ligand of the Ni complex remains attached unaltered to the Ni-core throughout the oxidation. Finally, the O-atom liberated from the encounter complex of the ion–molecule reactions (*Eqn. 2*) also stems specifically from molecular oxygen. Thus, O–O bond activation is crucial in the course of these reactions.

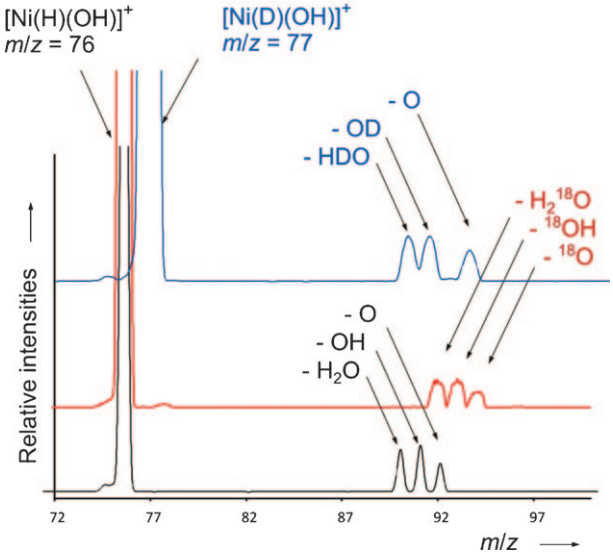

Fig. 1. *Thermal ion–molecule reactions of mass-selected [Ni(H)(OH)]⁺ with $^{16}O_2$* (black line), *[Ni(H)(OH)]⁺ with $^{18}O_2$* (red line), *and [Ni(D)(OH)]⁺ with $^{16}O_2$* (blue line) *at* $E_{lab} = 0$ *eV* (for experimental details, see [9])

While HO_2 can be formed by direct H-atom abstraction (*Scheme 2*, *Path a*), other product channels require the initial activation of both the Ni–H and the O–O bonds. To obtain mechanistic insight in this scenario, we decided to perform density-functional theory (DFT)-based calculations of the reaction network depicted in *Scheme 2*. Of special interest are questions related *i*) to the role of spin states[3]), *ii*) the actual pathways by which the conjectured hydroperoxide intermediates are generated, *i.e.*,

Scheme 2

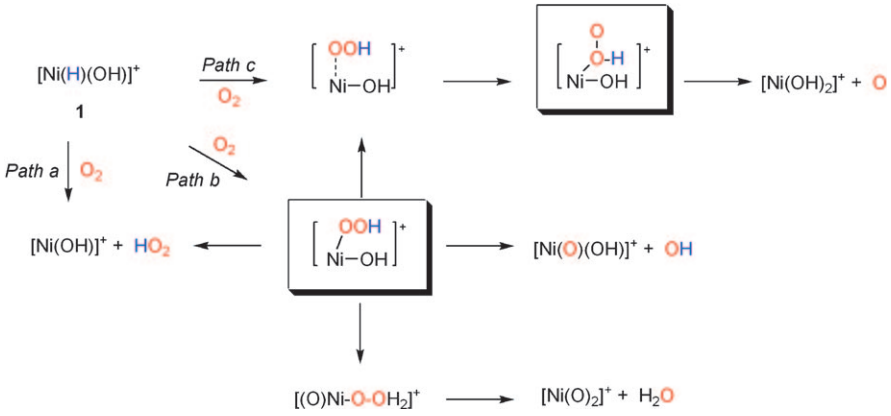

[3]) For review articles, see [10].

either directly (*Path b*) or *via* a loosely bound complex (*Path c*), and *iii*) insight on the isotope-specific generation of the neutral fragments H_2O, OH, and O, respectively (*Fig. 1*). Given the well-known limitations of DFT for a quantitatively correct description of open-shell, ligand-deficient transition-metal fragments [11], the computational findings reported here only aim at a qualitative analysis of the ion–molecule reactions depicted in *Scheme 2*.

Computational. – In the computational studies, the geometries of all species were optimized at the unrestricted UB3LYP level of theory [12] as implemented in the Gaussian03 programme package [13]. For the Ni-atom, the aug-cc-pVTZ-DK set [14] was used; for the O-atom, we employed the au-cc-pVTZ, and for the H-atom the cc-pVTZ basis sets [15]. Vibrational frequency analyses were performed at the same level of theory to characterize the nature of the stationary points as minima or transition structures, and to derive the zero-point energy (ZPE) and the entropy corrections (at 298 K). Intrinsic reaction coordinate (IRC) calculations were performed to link transition structures with the intermediates shown [16]. Whenever appropriate, the barrierless nature of association–dissociation paths were confirmed by linear scans along the reaction coordinate. The accuracy of our qualitative approach is in the order of $\pm$ 20 kJ mol^{-1} for relative energies of isomers [17]. The free energies (in kJ mol^{-1} in the *Figures*) are given relative to the free energy of the ground-state entrance channel, *i.e.,* O_2 (triplet) and $[Ni(H)(OH)]^+$ (quartet)[4]); relevant geometric data are given in Å (for bond lengths) and in degrees (for bond angles). In the non-equilibrium, gas-phase environment of the ion–molecule reactions, species with energies less than or equal to the free energies of the reactants are treated as accessible. While the dissociation paths forming fragmentation products are considered to be irreversible, rearrangements are regarded as reversible.

DFT, as shown by recent theoretical studies [5][20][21], is reliable enough to provide data consistent with experimental results and CCSD(T) calculations on similar systems. On the other hand, this performance is expected to decrease – as is well known – when the system under investigation has high multi-reference character. CCSD(T) and MCSCF calculations on $[Ni(H)(OH)]^+$ equilibrium structure confirm the reliability of DFT in this system as well [19]. Our approach in this work aims at an understanding of the potential energy surface (PES) within the limitations of DFT and leaving the points which need to be treated more thoroughly to a subsequent, higher-level theory work. Therefore, B3LYP instead of the computationally much more demanding *ab initio* tools was chosen for exploring the reaction mechanisms for the processes depicted in *Scheme 2*.

Results and Discussion. – 1. *Formation of HO_2 from $[Ni(H)(OH)]^+/O_2$.* Based on the simplified potential energy surface (PES; *Fig. 2*), the quartet state of $[Ni(H)(OH)]^+$ (^{4}**1**) forms the association complex ^{4}**2** in a spin-allowed, exothermic reaction. Next, in a practically barrier-free process, the H-atom transfer *via* ^{4}**TS$_{2-3}$** occurs to generate the separated products HO_2 and $[Ni(H)(OH)]^+$ (^{3}**3**) in an energetically rather downhill path. The changes in bond lengths, *Mulliken* charges, and spin densities in the course of the overall reaction do not exhibit any particular anomalies. We have also located a reaction path which proceeds on the doublet surface. While this process also occurs energetically below the entrance channel, the rather substantial energy difference between the transition states for the H-atom transfer on the doublet/quartet surfaces as well as the large triplet/singlet energy difference for the

---

4) For a detailed *ab initio* study on $[Ni,H_2,O]^+$ isomers, including $[Ni(H)(OH)]^+$ in different electronic states, see [18]. Recent state-of-the-art calculations [19] point to a rather complex electronic-structure situation of $[Ni(H)(OH)]^+$, an adequate, satisfying treatment of which requires extensive CCSD(T) or elaborate MRCAS calculations.

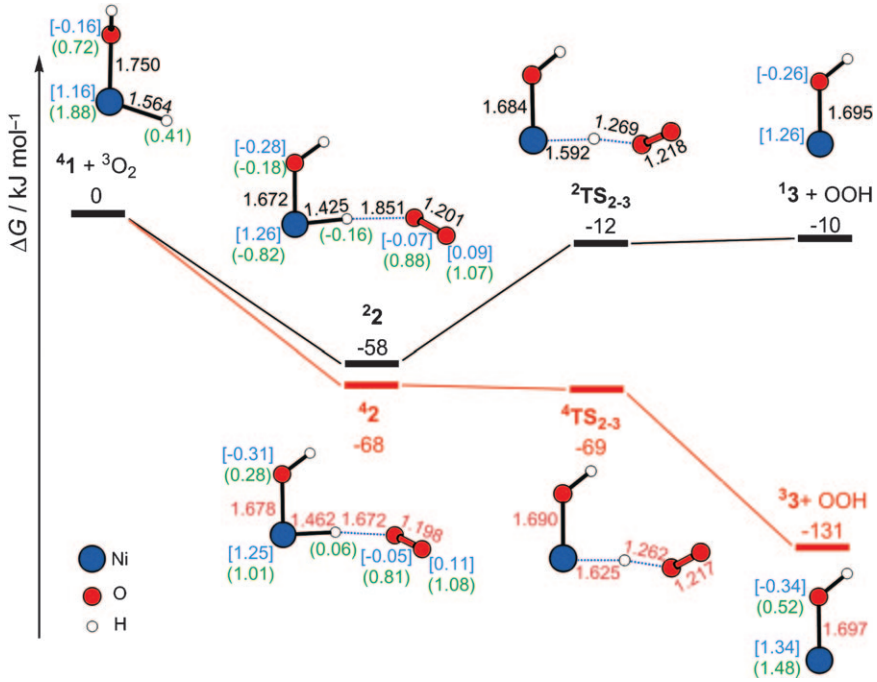

Fig. 2. *PES for the formation of [Ni,O,H]⁺ and HO_2*. Distances are given in Å, *Mulliken* charges (blue) and spin densities (green) are indicated in parentheses.

product ion $[Ni(OH)]^+$ (**^{1}3** *vs.* **^{3}3**) make the involvement of the doublet surface less likely.

2. *Pathways to the Nickel Hydroperoxide Intermediate [Ni(OH)(OOH)]⁺* (**5**): Direct interaction of $^3O_2$ with **^{4}1** can give rise to the exothermic, spin-allowed formation of the encounter complex **4** in its doublet, quartet, or sextet state (with decreasing exothermicity). Provided the surfaces lie close, and spin-orbit coupling (SOC) is high, the latter state, **^{6}4**, may also undergo spin-inversions to generate the energetically more favored quartet and doublet states **^{4}4** and **^{2}4**, respectively. While we did not find a transition structure for the rearrangement **^{6}4** → **^{6}5**, for the other spin states we succeeded in locating **^{2}TS$_{4-5}$** and **^{4}TS$_{4-5}$** with the latter being by 55 kJ mol^{-1} lower in energy (*Fig. 3*). The sextet state for a d^7 Ni^{III} complex is energetically much higher than the quartet and doublet states, and is, therefore, not considered any further in the discussion. At the DFT level, the two spin states of the hydroperoxide **5** are nearly isoenergetic as are their endothermic isomerizations to the isomers **^{2,4}6**. A great similarity exists also for the geometries (bond lengths) and charge distributions of **5**, **TS$_{5-6}$**, and **6** for either spin state, and a major difference concerns only the spin distributions in the OOH unit. As to the most likely reaction path, connecting the entrance channel with the oxygen-insertion products **5** and **6**, the DFT calculations clearly favor a preferred involvement of the quartet spin surface. This may include two crossings of the doublet and quartet surfaces before and after **^{2}TS$_{4-5}$** to utilize the more

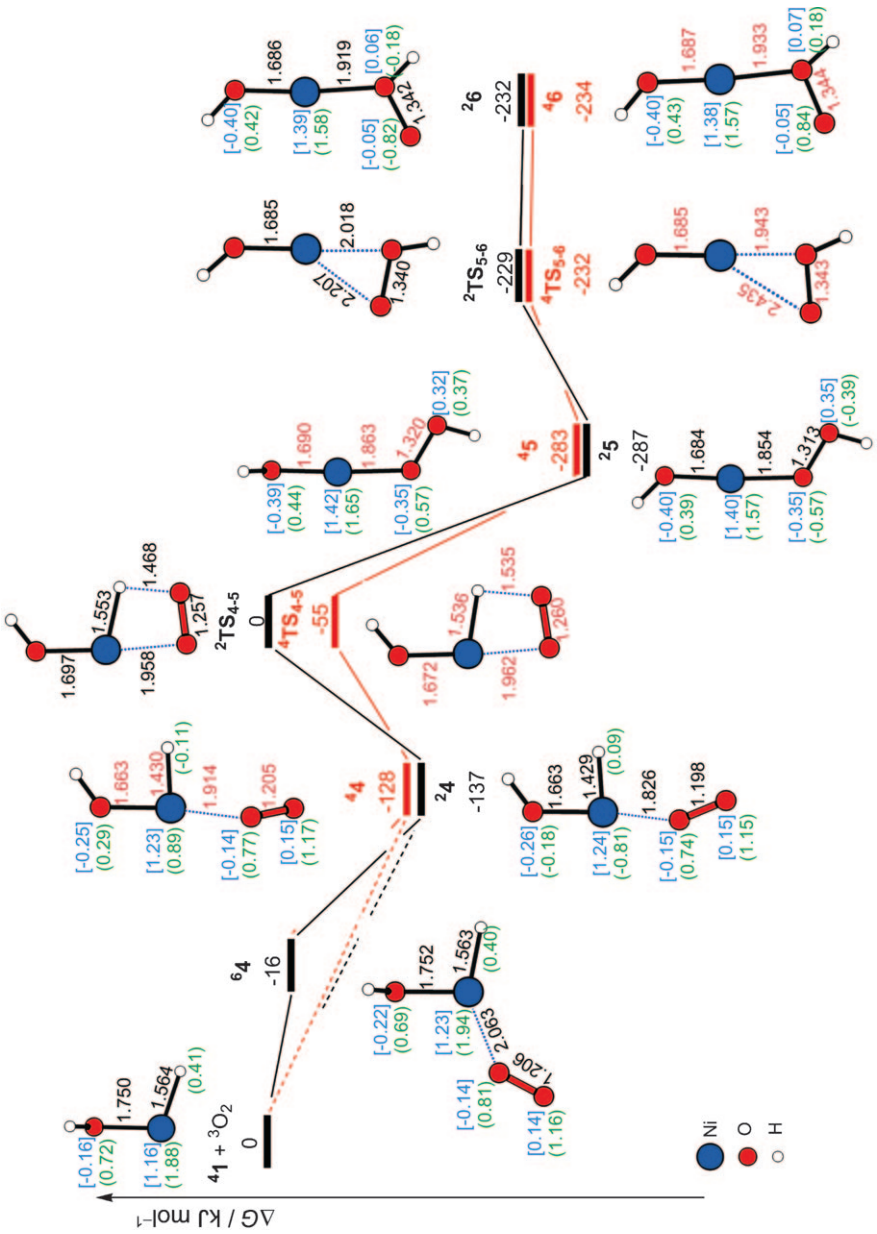

Fig. 3. *PES for the formation of* $[Ni(OH)(OOH)]^+$ *and its isomer* $[Ni(OH)(OHO)]^+$ (**6**)

feasible path going over ^{4}**TS**$_{4-5}$. In another alternative, **5** may form on the quartet surface and then decay to ^{2}**5**. Given the structural and energetic similarity of intermediates ^{2}**4** and ^{4}**4**, and ^{2}**5** and ^{4}**5** intersystem crossings (ISCs) at **4** and **5** can be expected.

3. *Elimination of H_2O from the Intermediate* **5**. As stated above, this reaction is quite prominent in the thermal activation of O_2 by $[Ni(H)(OH)]^+$ and occurs with high specificity with regard to the origin of the H_2O constituents. The DFT calculations (*Fig. 4*) suggest that the thermochemically preferred reaction will proceed on the doublet surface, because the nickel dioxide product cation ^{2}**8** is in its doublet state by 25 kJ mol^{-1} more stable than the analog quartet electromer ^{4}**8**. Moreover, formation of the latter is by 17 kJ mol^{-1} endothermic with respect to the entrance channel. However, a reversal of relative stabilities between the quartet/doublet states of the PES is encountered for both the transition state **TS**$_{5-7}$ as well as intermediate **7**; based on an analysis of the geometric data, the latter ion can be viewed as an ion–molecule association of cationic NiO^+ and water oxide[5]), rather than H_2O solvating $[Ni(O)_2]^+$. If the reaction were to preferentially proceed on the doublet surface, H_2O loss from ^{4}**7** to produce the product ^{2}**8** requires an SOC-mediated change of multiplicity. Alternatively, ^{4}**7** may constitute a dead-end of the isomerization, and the actual elimination of H_2O occurs adiabatically *via* the energetically accessible, though less favored, transition state ^{2}**TS**$_{5-7}$ to generate in a spin-conserving manner ^{2}**7**, and then its dissociation products $[Ni(O)_2]^+$ (^{2}**8**) and H_2O. Not surprisingly, given the unfavorable high Ni^V oxidation state, the nickel dioxide cations ^{2,4}**8** are thermochemically much less stable than the isomeric Ni^I–dioxygen complexes ^{2,4}**9**. Although the isomerization/dissociation route **7** → **TS**$_{7-9}$ → **9** + H_2O is energetically above the path ^{2}**7** → ^{2}**8**, it cannot be ruled out definitively.

4. *Liberation of OH from $[Ni(H)(OH)]^+/O_2$*. The isotope-labeling experiments (*Fig. 1*) leave no doubt as to the origin of OH generated from the $[Ni(H)(OH)]^+/O_2$ couple, in that the H-atom stems from the Ni–H bond, and the O-atom is provided by molecular oxygen. The already present OH group in the Ni complex $[Ni(H)(OH)]^+$ remains bound to the Ni-core. As will be shown, a satisfactory explanation of these experimental findings within the framework of the present calculations is beyond what DFT is capable to tell us. Based on the experimental results, a good starting point for the computational exercise is the insertion intermediate **5**, that can be formed in spin-allowed processes in its practically isoenergetic quartet and doublet states (*Fig. 3*). As indicated in *Fig. 5*, cleavage of the 'correct' O–OH bond in the doublet state ^{2}**5** to generate $[Ni(O)(OH)]^+$ (^{1}**10**) as well as to split the 'wrong' Ni–OH bond of ^{2}**5** to produce $[Ni(OOH)]^+$ (^{1}**11**) is thermodynamically too demanding on the ground that the two dissociation products are located above the reactants initial free energy. However, the situation looks completely different for the quartet hydroperoxide intermediate ^{4}**5**. Here, cleavage of both the O–OH and the Ni–OH bonds can proceed below the entrance channel with a clear energetic preference of the latter, *i.e.*, the bond is cleaved that leads to the 'wrong' isotope distribution. We have considered quite a few alternatives to resolve this dilemma. For example, while the absolute free-energy

---

[5]) For experimental and computational studies on the metal-free 'elusive' water oxide, H_2OO, see [22].

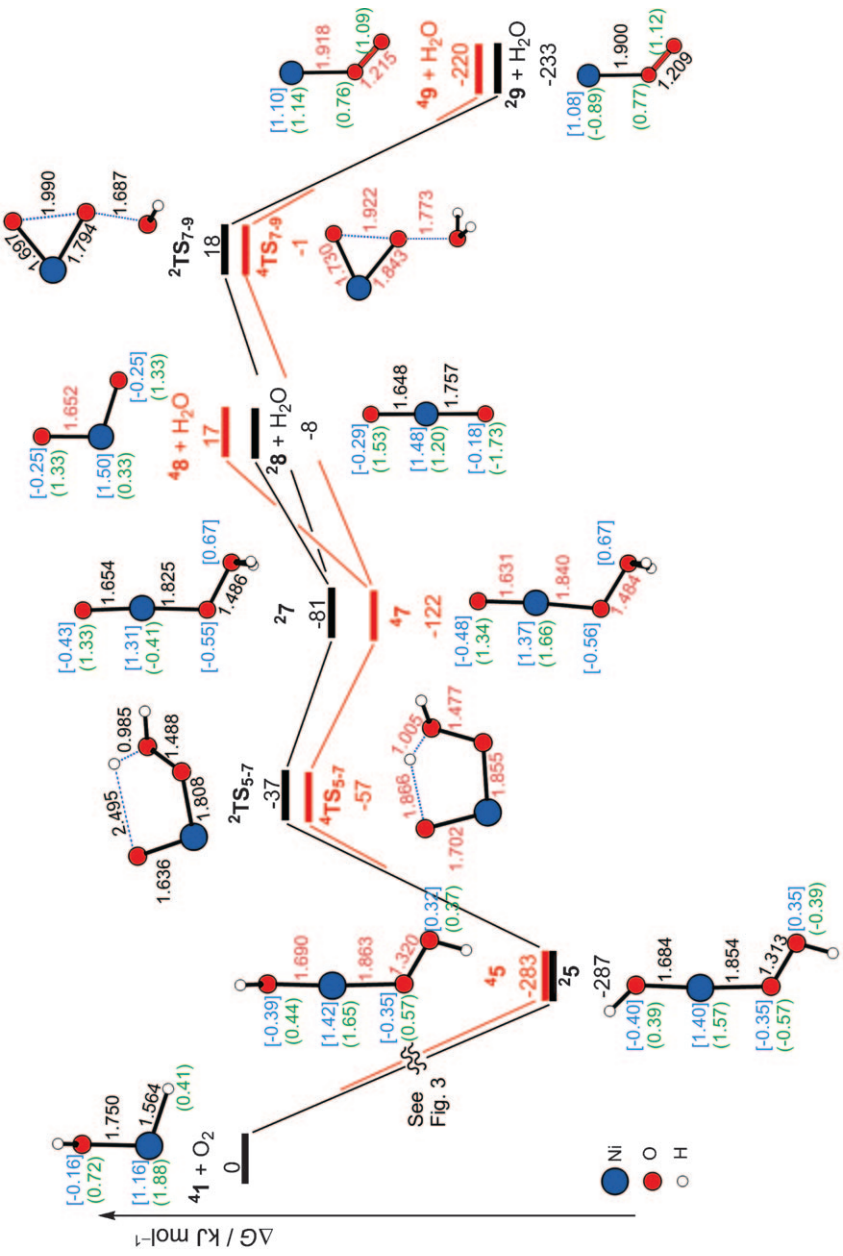

Fig. 4. *PES for the elimination of H_2O from $[Ni(OH)(OOH)]^+$* (**5**) *and the isomerization of $[Ni,O_2]^+$*

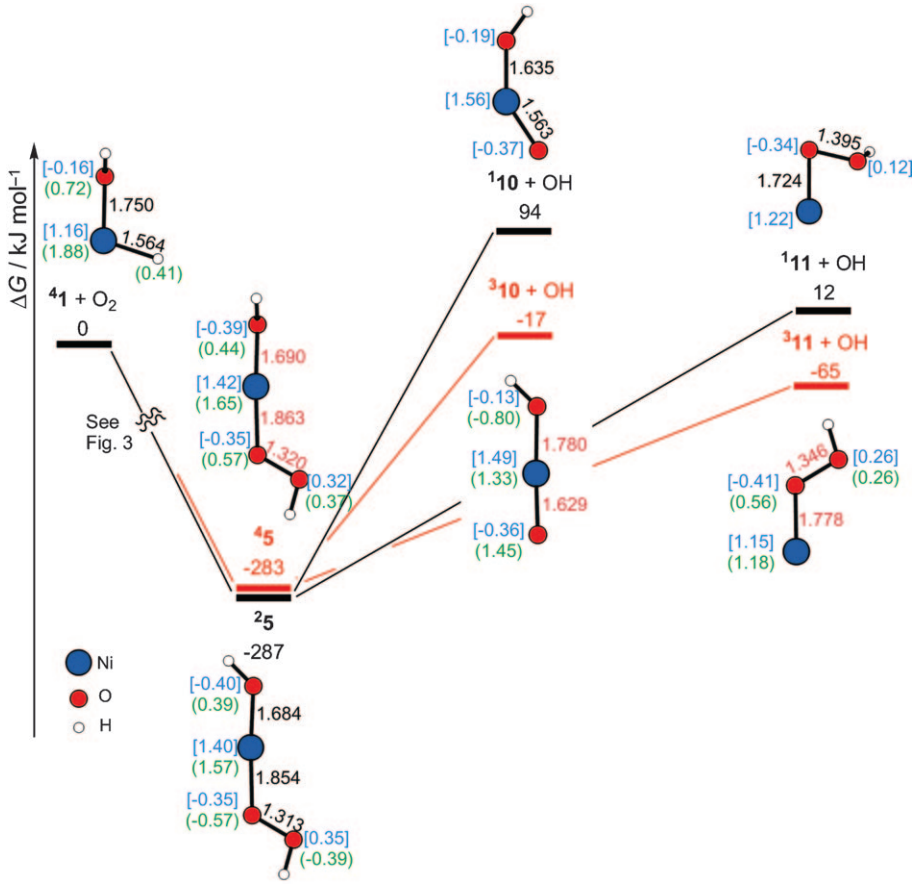

Fig. 5. *PES for the liberation of HO from [Ni(H)(OH)]⁺/O₂*

differences of **³10** (the 'correct' product) *vs.* the more stable isomer **³11** (the 'wrong' product) may vary by using different DFT functionals or by employing *ab initio*-based calculations, their relative energetic ordering is not likely to change given the fact that Ni prefers the formal oxidation state +II (as in **11**) *vs.* the +IV state as in **10**. Next, we have searched for alternative pathways to link **⁴5** with products that are compatible with the isotope distribution obtained experimentally. While the PES is rather rich and complex, we did not manage to locate a path that would resolve the discrepancy. Further, an analysis of the change of spin densities in the course of OH formation from $[Ni(OH)(OOH)]^+$ (**⁴5**) is also of no avail, because the electronic reorganization in breaking either the 'correct' O–OH or the 'wrong' Ni–OH bonds are comparable in that the spin densities of the O-atoms in question change in a comparable manner, *i.e.*, from 0.37 (for the former) or 0.44 (for the latter scenario) to 1.0. If there is a 'hidden' barrier in the process **⁴5** → **³11** + OH, it obviously cannot be uncovered by DFT. Moreover, severe spin contamination in **³10** with $\langle S^2 \rangle = 2.79$ points to the need to

further elaborate the electronic structures of the species of the PES as we are facing a situation which indicates the limitations of the DFT-based approach employed[6]).

5. *O-Atom Formation from* $[Ni(H)(OH)]^+/O_2$. As mentioned earlier [9], this reaction is also site-specific and involves an O-atom provided by the incoming O_2 molecule; this experimental finding fits well with the DFT calculations (*Fig. 6*). As an obvious candidate for a starting point, we considered intermediate **6** which, in two different spin states, is accessible from $[Ni(H)(OH)]^+$ (^{4}**1**) and O_2 (*Fig. 3*). For either spin state of **6**, expulsion of O-atom proceeds in spin-allowed processes by splitting the O–O(H) bond to generate the Ni^{III} dihydroxide cation **12**. Both spin isomers ^{2}**12** and ^{4}**12** are located below the entrance channel and are, therefore, accessible in the experiment. The isomerization ^{2,4}**12** $\rightleftarrows$ ^{2,4}**13**, *i.e.*, the mutual conversion of a Ni^{III} dihydroxide to a Ni^{III} oxide, 'solvated' by a H_2O molecule, is not likely to occur under thermal conditions given the rather energy-demanding transition states ^{2,4}**TS$_{12-13}$** that connects the two isomers **12** and **13** (*Fig. 6*).

6. *The O_2-Catalyzed Isomerization $[Ni(H)(OH)]^+ \rightarrow [Ni(H_2O)]^+$*. Extensive computational studies have demonstrated that the $[Ni(H_2O)]^+$ complex, in its doublet state, corresponds to the global minimum of the $[Ni,H_2,O]^+$ PES [18], and providing an answer to the obvious question why isomerization of the rather energy-rich quartet state of $[Ni(H)(OH)]^+$ (^{4}**1**) does not occur efficiently on the time scale of the experiment [8][9] will form the subject of a forthcoming detailed theoretical study [19]. Here, we would like to mention, that – in addition to the unimolecular isomerization $[Ni(H)(OH)]^+$ (^{4}**1**) $\rightarrow$ $[Ni(H_2O)]^+$ (^{2}**14**) – there exists also an O_2-catalyzed, bimolecular variant, at least according to the DFT calculations (*Fig. 7*). The starting point corresponds to the quartet and doublet states of the easily formed hydroperoxide insertion intermediate **5**; with regard to its isomerization, this species has at least three options. On both the quartet and doublet surfaces, we located a direct path ^{4}**5** $\rightarrow$ **TS$_{5-14}$** $\rightarrow$ ^{2}**14** + ^{3}**O$_2$** as well as the more complex route **5** $\rightarrow$ **6** $\rightarrow$ **TS$_{6-14}$** $\rightarrow$ ^{2}**14** + ^{3}**O$_2$**, with a clear energetic preference for the former. IRC Calculation and an analysis of the imaginary vibrations of **TS$_{5-14}$** and **TS$_{6-14}$** demonstrate the formation of O_2 and H_2O *via* a H-atom transfer from OOH to the OH moiety. However, it is interesting that no $[H_2O \cdots Ni \cdots O_2]^+$ intermediate could be located computationally. Rather, the transition states ^{2,4}**TS$_{5-14}$** lead to a direct expulsion of O_2. When the triplet dioxygen departs from ^{2,4}**TS$_{5-14}$** the two d spins of O_2 can either be coupled parallel or antiparallel to the total spins in the resulting $[Ni(H_2O)]^+$ complex ^{2}**14**. Therefore, the formation of the product combination ^{2}**14** + $^3O_2$ is a spin-allowed process in both the quartet and doublet states. Both the O_2-catalyzed, exothermic isomerization $[Ni(H)(OH)]^+ \rightarrow [Ni(H_2O)]^+$ and the easy access to various dissociation channels (*Figs. 2–6*) may explain the absence of a signal for a long-lived adduct complex $[Ni(H)(OH)]^+/O_2$ in *Fig. 1*.

Conclusions. – DFT-Based calculations were employed – as a first approach – to investigate the rich, complex, and yet highly specific chemistry in the gas-phase reactions of $[Ni(H)(OH)]^+$ with molecular oxygen. A qualitative framework to

---

[6]) We should like to point out that, in the otherwise extensive DFT analysis [5] of the related triplet/singlet dichotomy of various $L_nPd(H)(X)/O_2$ systems, a thorough analysis of this fundamental problem has not been included.

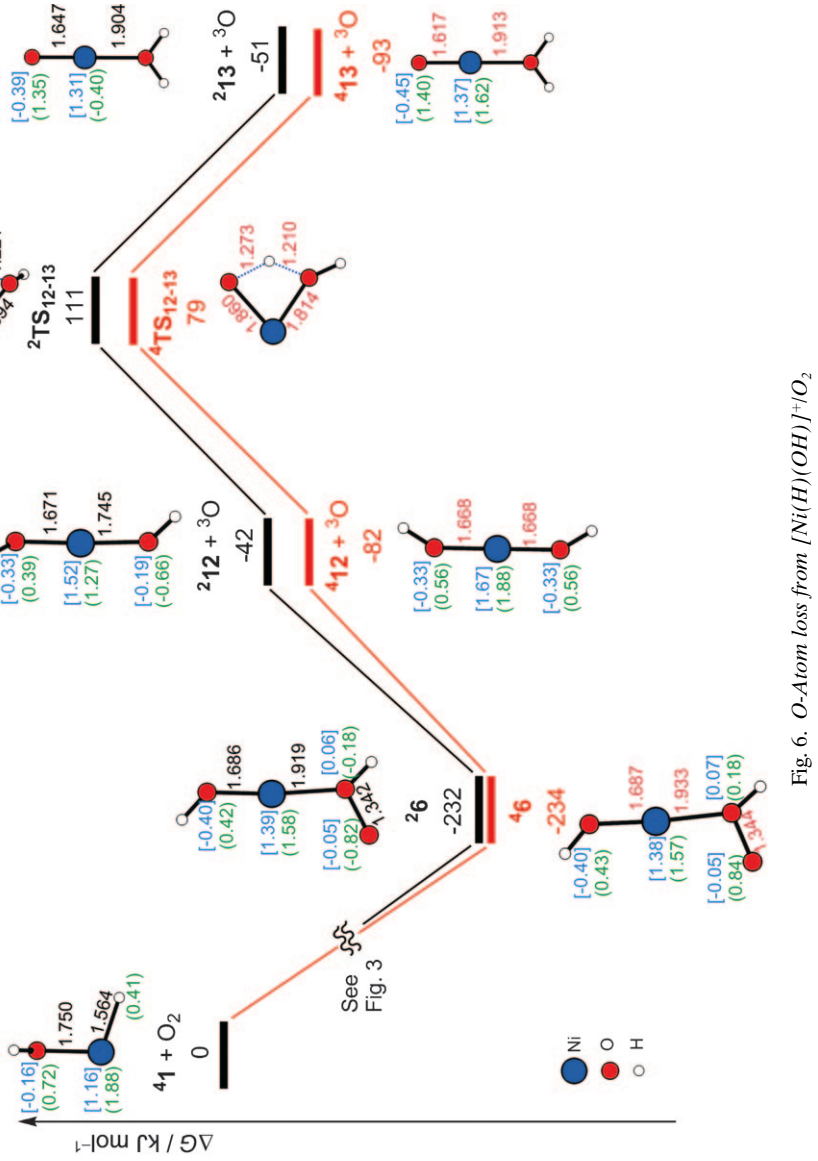

Fig. 6. *O-Atom loss from* $[Ni(H)(OH)]^{+}/O_2$

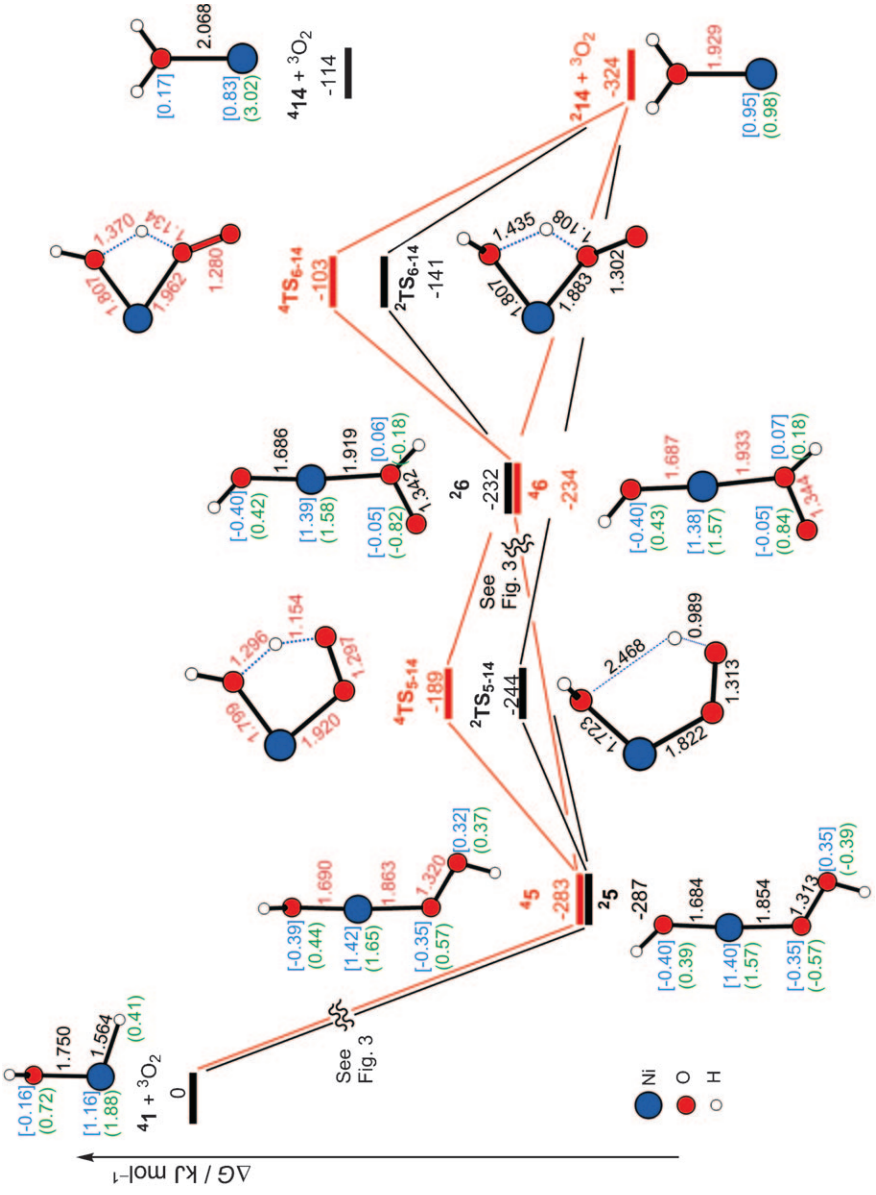

Fig. 7. *O_2-Catalyzed isomerization paths for $[Ni(H)(OH)]^+ \rightarrow [Ni(H_2O)]^+$, based on DFT calculations*

understand the reaction mechanism has been established. The calculations reveal that *i*) both direct H-abstraction as well as a dioxygen-insertion pathway are feasible as the first steps. *ii*) The fragmentations to liberate O, OH, and H_2O are likely to start from the low-energy hydroperoxide intermediates **5** and **6**. *iii*) Transition structures and barrier-free fragmentation channels lying below the entrance free energy and leading to the experimentally observed products were presented. *iv*) A major reaction path corresponds to the O_2-catalyzed, exothermic isomerization of $[Ni(H)(OH)]^+$ to $[Ni(OH_2)]^+$. Finally, while the current DFT study sheds light on many facets of this interesting system, some crucial points are still unexplained, such as aspects of crossings between spin states and the magnitude of nonadiabatic coupling between surfaces. More detailed calculations to address those issues are in progress.

Financial support of this work by the *Fonds der Chemischen Industrie* and by the *Cluster of Excellence 'Unifying Concepts in Catalysis'*, coordinated by the Technische Universität Berlin and funded by the *Deutsche Forschungsgemeinschaft*, is appreciated. *X. Z.* is grateful to the *Alexander von Humboldt-Stiftung* for a postdoctoral fellowship. *Y. D.* thanks the *Scientific and Technological Research Council of Turkey* for a *TÜBITAK* postdoctoral fellowship.

REFERENCES

[1] S. S. Stahl, *Angew. Chem., Int. Ed.* **2004**, *43*, 3400; S. S. Stahl, *Science* **2005**, *309*, 1824.
[2] K. M. Gligorich, M. S. Sigman, *Angew. Chem., Int. Ed.* **2006**, *45*, 6612.
[3] M. C. Denney, N. A. Smythe, K. L. Celto, R. A. Kemp, K. I. Goldberg, *J. Am. Chem. Soc.* **2006**, *128*, 2508; M. M. Konnick, B. A. Gandhi, I. A Guzei, S. S. Stahl, *Angew. Chem., Int. Ed.* **2006**, *45*, 2904.
[4] T. Mosokowa, S.-I. Musabashi, *Acc. Chem. Res.* **1990**, *23*, 49.
[5] R. Prabhakar, P. E. M. Siegbahn, B. F. Minaev, H. Ågren, *J. Phys. Chem., B* **2002**, *106*, 3742; C. R. Landis, C. M. Morales, S. S. Stahl, *J. Am. Chem. Soc.* **2004**, *126*, 16302; T. Privalov, C. Linde, K. Zetterberg, C. Moberg, *Organometallics* **2005**, *24*, 885; J. M. Keith, R. J. Nielsen, J. Oxgaard, W. A. Goddard III, *J. Am. Chem. Soc.* **2005**, *127*, 13172; J. M. Keith, R. P. Muller, R. A. Kemp, K. I. Goldberg, W. A. Goddard III, J. Oxgaard, *Inorg. Chem.* **2006**, *45*, 9631; S. Chowdhury, I. Rivalta, N. Russo, E. Sicilia, *Chem. Phys. Lett.* **2007**, *443*, 183; J. M. Keith, W. A. Goddard III, J. Oxgaard, *J. Am. Chem. Soc.* **2007**, *129*, 10361; B. V. Popp, S. S. Stahl, *J. Am. Chem. Soc.* **2007**, *129*, 4410.
[6] J. H. Bayston, R. N. Beale, N. K. King, M. E. Winfield, *Aust. J. Chem.* **1963**, *16*, 954; J. H. Bayston, M. E. Winfield, *J. Catal.* **1964**, *3*, 123; H. L. Roberts, W. R. Symes, *J. Chem. Soc., A* **1968**, 1450; L. E. Johnstone, J. A. Page, *Can. J. Chem.* **1969**, *47*, 4241; R. D. Gillard, B. T. Heaton, D. H. Vaughan, *J. Chem. Soc., A* **1970**, 3126; J. F. Endcott, C.-L. Wong, T. Inour, P. Natarajan, *Inorg. Chem.* **1979**, *18*, 450; M. T. Atlay, M. Preece, G. Strukul, B. R. James, *Can. J. Chem.* **1983**, *61*, 1332; A. Bakac, *J. Am. Chem. Soc.* **1997**, *119*, 10726; D. D. Wick, K. I. Goldberg, *J. Am. Chem. Soc.* **1999**, *121*, 11900; S. Thyagaran, C. D. Incarvito, A. L. Rheingold, K. H. Theopold, *Chem. Commun.* **2001**, 2198.
[7] R. R. Squires, *Chem. Rev.* **1987**, *87*, 623; C. E. C. A. Hop, T. B. McMahon, *J. Am. Chem. Soc.* **1992**, *114*, 1237; D. Schröder, H. Schwarz, *Angew. Chem., Int. Ed.* **1993**, *32*, 1420; P. Boissel, P. Marty, A. Klotz, P. de Parseval, B. Candret, G. Serra, *Chem. Phys. Lett.* **1995**, *242*, 157; A. Fiedler, I. Kretzschmar, D. Schröder, H. Schwarz, *J. Am. Chem. Soc.* **1996**, *118*, 9941; M. Pavlov, M. R. A. Blomberg, P. E. M. Siegbahn, R. Wesendrup, C. Heinemann, H. Schwarz, *J. Phys. Chem., A* **1997**, *101*, 1567; D. Schröder, H. Schwarz, 'Essays in Contemporary Chemistry: From Molecular Structure towards Biology', Eds. G. Quinkert, M. V. Kisakürek, Verlag Helvetica Chimica Acta, Basel, Wiley-VCH, Weinheim, 2001, p. 131; M. Brönstrup, D. Schröder, I. Kretzschmar, H. Schwarz, J. N. Harvey, *J. Am. Chem. Soc.* **2001**, *123*, 142; G. K. Koyanagi, D. K. Böhme, I. Kretzschmar, D. Schröder, H. Schwarz, *J. Phys. Chem., A* **2001**, *105*, 4259; M. Engeser, T. Weiske, D. Schröder, H. Schwarz, *J. Phys. Chem., A* **2003**, *107*, 2855; L. D. Socacin, J. Hagen, T. M. Bernhardt, L. Wöste, U. Heiz, H. Häkkinen, U. Landmann, *J. Am. Chem. Soc.* **2003**, *125*, 10437; K. Koszinowski, D. Schröder, H. Schwarz, *ChemPhysChem* **2003**, *4*, 1233; K. Koszinowski, D. Schröder, H. Schwarz, *J. Phys. Chem., A* **2003**, *107*,

4999; M. L. Kimble, A. W. Castleman Jr., R. Mitrić, C. Bürgel, V. Bonačić-Koutecký, *J. Am. Chem. Soc.* **2004**, *126*, 2526; L. Operti, R. Rabezzana, *Mass Spectrom. Rev.* **2006**, *25*, 483; F. Xia, Z. Cao, *Organometallics* **2007**, *26*, 16098; S. Feyel, D. Schröder, H. Schwarz, *Eur. J. Inorg. Chem.* **2008**, 4961; D. Schröder, H. Schwarz, *Proc. Natl. Acad. Sci. U.S.A.* **2008**, *105*, 18114; R. Burgert, H. Schnöckel, A. Grubusic, X. Li, S. T. Stokes, K. H. Bowen, G. F. Ganteför, B. Kiran, P. Jena, *Science* **2008**, *319*, 438.

[8] M. Schlangen, D. Schröder, H. Schwarz, *Angew. Chem., Int. Ed.* **2007**, *46*, 1641.

[9] M. Schlangen, H. Schwarz, *Helv. Chim. Acta* **2008**, *91*, 379.

[10] P. B. Armentrout, *Science* **1991**, *251*, 175; J. C. Weisshaar, *Acc. Chem. Res.* **1993**, *26*, 213; D. A. Plattner, *Angew. Chem., Int. Ed.* **1999**, *38*, 82; D. Schröder, S. Shaik, H. Schwarz, *Acc. Chem. Res.* **2000**, *33*, 139; R. Poli, J. N. Harvey, *Chem. Soc. Rev.* **2003**, *32*, 1; H. Schwarz, *Int. J. Mass Spectrom.* **2004**, *237*, 75; J. M. Mercero, J. M. Matxain, X. Lopez, D. M. York, A. Largo, L. A. Erikson, J. M. Ugalde, *Int. J. Mass Spectrom.* **2005**, *240*, 37; I. Rivalta, N. Russo, E. Sicilia, *J. Comput. Chem.* **2006**, *27*, 174; B. K. Carpenter, *Chem. Soc. Rev.* **2006**, *35*, 736; J. N. Harvey, *Phys. Chem. Chem. Phys.* **2007**, *9*, 331; S. Shaik, H. Hirao, D. Kumar, *Acc. Chem. Res.* **2007**, *40*, 532; M. Neumaier, R. Köppe, H. Schnöckel, *Nachr. Chem. Tech. Lab.* **2008**, *56*, 999.

[11] 'Transition State Modeling for Catalysis', in 'ACS Symposium Series, Vol. 721', Eds. D. G. Truhlar, K. Morokuma, American Chemical Society, Washington, D. C., 1988; W. Koch, M. C. Holthausen, 'A Chemist's Guide to Density Functional Theory', Wiley-VCH, Weinheim, 2000; 'Computational Organometallic Chemistry', Ed. T. R. Cundari, Marcel Dekker, New York, 2001; P. Schreiner, *Angew. Chem., Int. Ed.* **2007**, *46*, 4217; S. Feyel, J. Döbler, R. Höckendorf, M. K. Beyer, J. Sauer, H. Schwarz, *Angew. Chem., Int. Ed.* **2008**, *47*, 1946; Y. Zhao, D. G. Truhlar, *Acc. Chem. Res.* **2008**, *41*, 157; 'Computational Modeling for Homogeneous and Enzymatic Catalysis. A Knowledge-Base for Designing Efficient Catalysts', Eds. K. Morokuma, D. Musaev, Wiley-VCH, Weinheim, 2008.

[12] C. Lee, W. Yang, R. G. Parr, *Phys. Rev. B: Condens. Matter* **1988**, *37*, 785; A. D. Becke, *J. Chem. Phys.* **1993**, *98*, 5648.

[13] M. J. Frisch, G. W. Trucks, H. B. Schlegel, G. E. Scuseria, J. R. C. M. A. Robb, J. A. Montgomery Jr., T. Vreven, J. C. B. K. N. Kudin, J. M. Millam, S. S. Iyengar, J. Tomasi, B. M. V. Barone, M. Cossi, G. Scalmani, N. Rega, H. N. G. A. Petersson, M. Hada, M. Ehara, K. Toyota, J. H. R. Fukuda, M. Ishida, T. Nakajima, Y. Honda, O. Kitao, M. K. H. Nakai, X. Li, J. E. Knox, H. P. Hratchian, J. B. Cross, J. J. C. Adamo, R. Gomperts, R. E. Stratmann, O. Yazyev, R. C. A. J. Autin, C. Pomelli, J. W. Ochterski, P. Y. Ayala, G. A. V. K. Morokuma, P. Salvador, J. J. Dannenberg, S. D. V. G. Zakrezewski, A. D. Daniels, M. C. Strain, D. K. M. O. Farkas, A. D. Rabuck, K. Raghavachari, J. V. O. J. B. Foresman, Q. Cui, A. G. Baboul, S. Clifford, B. B. S. J. Cioslowski, G. Liu, A. Liashenko, P. Piskorz, R. L. M. I. Komaromi, D. J. Fox, T. Keith, M. A. Al-Laham, A. N. C. Y. Peng, M. Challacombe, P. M. W. Gill, and W. C. B. Johnson, M. W. Wong, C. Gonzalez, J. A. Pople, Gaussian03, Revision C.02., *Gaussian Inc.*, Wallingford, 2004.

[14] N. B. Balabanov, K. A. Peterson, *J. Chem. Phys.* **2005**, *123*, 064107.

[15] T. H. Dunning Jr., *J. Chem. Phys.* **1989**, *90*, 1007.

[16] K. Fukui, *J. Phys. Chem.* **1970**, *74*, 4161; K. Fukui, *Acc. Chem. Res.* **1981**, *14*, 363; C. Gonzales, H. B. Schlegel, *J. Phys. Chem.* **1990**, *94*, 5523.

[17] M. C. Holthausen, A. Fiedler, H. Schwarz, W. Koch, *Angew. Chem., Int. Ed.* **1995**, *34*, 2282.

[18] A. Irigoras, O. Elizalde, I. Silanes, J. E. Fowler, J. M. Ugalde, *J. Am. Chem. Soc.* **2000**, *122*, 114.

[19] Y. Dede, M.-H. Baik, X. Zhang, M. Schlangen, H. Schwarz, in preparation.

[20] A. Luna, M. Alcamí, O. Mó, M. Yáñez, J. Tortajada, *Int. J. Mass Spectrom.* **2002**, *217*, 119; D. Herebian, K. E. Wieghardt, F. Neese, *J. Am. Chem. Soc.* **2003**, *125*, 10997; Y. Ohnishi, Y. Nakao, H. Sato, S. Sakaki, *J. Phys. Chem., A* **2007**, *111*, 7915; C. C. Lu, E. Bill, T. Weyhermüller, E. Bothe, K. Wieghardt, *J. Am. Chem. Soc.* **2008**, *130*, 3181.

[21] B. F. Gherman, M.-H. Baik, S. J. Lippard, R. A. Friesner, *J. Am. Chem. Soc.* **2004**, *126*, 2978; S. Yao, E. Bill, C. Milsmann, K. Wieghardt, M. Driess, *Angew. Chem., Int. Ed.* **2008**, *47*, 7110; L. W. Chung, X. Li, H. Sugimoto, Y. Shiro, K. Morokuma, *J. Am. Chem. Soc.* **2008**, *130*, 12299.

[22] D. Schröder, C. A. Schalley, N. Goldberg, J. Hrušák, H. Schwarz, *Chem. – Eur. J.* **1996**, *2*, 1235; C. A. Schalley, J. N. Harvey, D. Schröder, H. Schwarz, *J. Phys. Chem., A* **1998**, *102*, 1021.

Received November 14, 2008